

phys. stat. sol. (b) **56**, 223 (1973)

Subject classification: 6 and 20.1; 1.1; 12.2; 22.1.3

Max-Planck-Institut für Festkörperforschung, Stuttgart

Hydrostatic Pressure Dependence of First-Order Raman Frequencies in Se and Te

By

W. RICHTER, J. B. RENUCCI¹⁾, and M. CARDONA

Measurements of the effect of hydrostatic pressure on the first order Raman frequencies of Se and Te are reported. All the frequencies of the Raman active modes decrease with pressure. The valence force field model proposed by Nakayama and Odajima is used to explain this behaviour.

Es wird über Messungen des Einflusses eines hydrostatischen Drucks auf die Raman-frequenzen erster Ordnung von Se und Te berichtet. Alle Frequenzen der Raman-aktiven Moden nehmen mit dem Druck ab. Das von Nakayama und Odajima vorgeschlagene Valenzkraftfeldmodell wird zur Erklärung dieses Verhaltens benutzt.

1. Introduction

The shifts of the first order Raman lines of a number of diamond and zincblende crystals as a function of hydrostatic pressure have been measured [1 to 3]. For all of them the frequencies increase when applying pressure. However, calculations performed on Ge [4 to 6] and Si [6] show that the Grüneisen parameters of the TA phonons become negative at the edge of the Brillouin Zone. Measurements on Ge by Payne [7] for the TA phonon at the L-point of the Brillouin Zone give a negative Grüneisen parameter thus confirming the calculations. A similar result was found by Weinstein et al. [8] for the TA phonon of GaP at the X-point. Also, the low frequency ($q = 0$) E_2 -modes of wurtzite-type crystals like CdS and ZnO decrease with pressure [2]. This behaviour was explained by the fact that the wurtzite structure is related to the zincblende structure: the low-frequency zone centre E_2 -mode of the wurtzite structure corresponds to the L-point transverse acoustical mode at the zone boundary of the zincblende structure. Other crystal structures can be related to cubic structures in a similar way. For example, the dispersion curves of the phonon frequencies of trigonal Se and Te with three atoms per primitive cell are well reproduced if one thinks of the structures of these materials in terms of a distorted simple cubic lattice with one atom per unit cell [9, 10]. In this picture the $q = 0$ phonons of Se and Te correspond to acoustical phonons of the simple cubic lattice in the (111) direction $2/3$ of the Brillouin Zone away from the centre. One therefore might also expect for these phonon frequencies in Se and Te negative shifts when applying hydrostatic pressure. Negative values of the thermal expansion coefficient of Te also indicate the necessity of negative Grüneisen parameters [11, 12].

¹⁾ Permanent address: Laboratoire de physique expérimentale, Université Paul Sabatier, 31 Toulouse, France.

SEP 11 1973

We therefore undertook an investigation of the hydrostatic pressure dependence of the Raman frequencies in Se and Te. The unit cell of trigonal Se and Te contains three atoms arranged in a characteristic spiral chain. Five of the six optical modes are Raman active: one is of type A_1 and is solely Raman active, the two doubly degenerate type E vibrations are also infrared active (for a review see [13]). We shall denote the low-frequency E-mode E' and the high frequency E-mode E'' . The last mode, of symmetry A_2 , is only infrared active. The sequence of phonon frequencies in increasing order is for Se: A_2 , E' , E'' , A_1 and for Te: A_2 , E' , A_1 , E'' : the ordering of the E'' and A_1 is reverse in Se and Te. In this work we study the three Raman-active phonon frequencies under hydrostatic pressure in both materials.

The experimental arrangement is described in Section 2. The results, which show indeed a negative behaviour for the Grüneisen constants, are given in Section 3. A qualitative explanation is given in Section 4 on the basis of a simple model which relates the phonon frequencies of Se and Te. More quantitative results obtained on the basis of a valence force field model developed by Nakayama and Odajima [14] are also presented.

2. Experiment

The Se sample was a vapour grown needle and the Te sample was cut from a single crystal and etch polished [15]. The faces measured had (10 $\bar{1}$ 0) orientation. The samples were placed in a hydrostatic pressure cell of the type described by Brafman et al. [16]. The maximum pressure which could be obtained was 8 kbar. The backscattering configuration described by Buchenauer et al. [3] was employed since the samples are opaque to the exciting laser lines used. This arrangement produces a large amount of diffuse scattered light. In order to reduce it we chose long wavelength excitation. The 7525 Å line of a Kr^+ -laser was used for Se and the 6471 Å line of the same laser for Te to

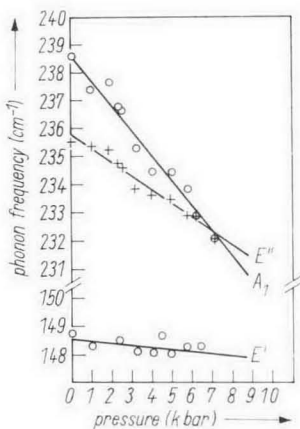


Fig. 1

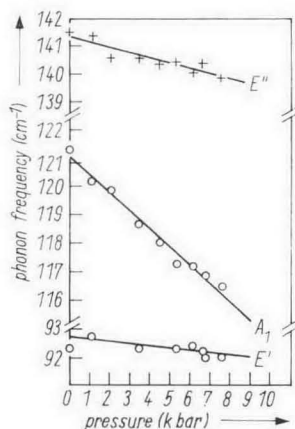


Fig. 2

Fig. 1. Frequency shift as a function of pressure for the first order Raman-active phonons in Se. The solid lines are least-square fits to the experimental points

Fig. 2. Frequency shift as a function of pressure for the first order Raman-active phonons in Te. The solid lines are least-square fits to the experimental points

approach as well as possible the conditions of resonance for these materials [17]. As some of the phonon frequencies are relatively low we used in addition a Spex triple monochromator to reduce stray light. All the shifts were measured relative to the position of a reference line produced by a neon lamp.

3. Results

The measured pressure dependence of the three Raman active phonon frequencies in Se and Te is shown in Fig. 1 and 2. The data can be summarized as follows: (i) For all modes the frequencies decrease with increasing pressure, the pressure coefficients $\alpha_i = d\omega_i/dp$ (see Table 1) being negative. (ii) The pressure coefficients are different for each mode, but similar for modes of the same symmetry in Se and Te. (iii) The coefficients for the E'-mode are much smaller than the ones for the A₁, E'' modes which are of comparable magnitude. The following relation holds for both Se and Te:

$$|\alpha(A_1)| > |\alpha(E'')| \gg |\alpha(E')|.$$

An important point to note is that the higher $|\alpha|$ for the A₁-mode pushes the frequency of this mode in Se below the E''-mode with increasing pressure. Thus by pressure application in Se the same frequency ordering of the modes is obtained as in Te. This fact, and the similar magnitudes of α in Se and Te, suggest the idea that one can obtain an approximation to the spectrum of Te by applying hydrostatic pressure to Se. This idea will be worked out in detail in the next section.

Table 1
Pressure coefficients (cm⁻¹/kbar) of phonon frequencies of Se and Te

modes	Se		Te	
	exp.	cal.	exp.	cal.
A ₁	-0.90	-0.59	-0.64	-0.75
E''	-0.49	-0.56	-0.19	-0.16
E'	-0.07	+0.05	-0.07	-0.51
A ₂		+0.51		+0.22

4. Discussion

The different physical behaviour of Se and Te can be interpreted in terms of the ratio between intra- and interchain bonding (see, for instance, [13]). Se behaves more like a molecular crystal with weak bonding force constants between the chains, whereas in Te the intra- and interchain force constants are of the same order (see Table 2). This has been shown in a number of valence force field calculations [12, 14, 18 to 20]. It manifests itself also in the behaviour of the elastic constants: the values of C_{33} and C_{13} , mainly determined by intrachain forces, are nearly equal in Se and Te, whereas the values of C_{11} , C_{12} , C_{14} , and C_{44} , governed by interchain forces, are twice larger in Te [23].

The lattice parameters of Se and Te show the same trends (Table 3). The ratio of the interchain distance a to the nearest neighbour distance in the chain r_0 is also bigger in Se than in Te thus implying more isolated chains in Se. (The

Table 2

Force constants (10^5 dyn/cm) and changes in force constants with pressure (10^5 dyn/cm kbar) in Se and Te. K_R is an interchain force constant. The remaining constants represent intrachain interactions.

	K_r	K_θ	$K_{rr'}$	$K_{r\theta}$	K_R
Se	1.18 ^{a)}	0.179 ^{a)}	0.045 ^{a)}	0.012 ^{a)}	0.046 ^{a)}
Te	0.707 ^{b)}	0.110 ^{b)}	0.131 ^{b)}	0.113 ^{c)}	0.164 ^{b)}
$\left(\frac{dK}{dp}\right)$ Se, Te	-0.0043 ^{c)}	-0.0006 ^{c)}	+0.0007 ^{c)}	+0.0009 ^{c)}	+0.0010 ^{c)}

a) From [14]; b) from [20]; c) present work.

absolute values of a , r_0 , and the lattice constant c along the trigonal axis are, of course, bigger in Te because of the greater size of the Te atoms.) In the light of the above remarks we tried to describe the difference in the phonon frequencies of Se and Te by the difference of the interchain distance a normalized to the nearest neighbour distance r_0 taking, of course, into account the different masses.

X-ray measurements under hydrostatic pressure in Se and Te show that a decreases with increasing pressure, while c increases only by a small amount [21, 22]. The main effect of hydrostatic pressure is then to move the chains closer together. No information is available about the variation of the internal parameter r_0 or θ (bond angle) with hydrostatic pressure. If one assumes small angle changes with pressure, the change in c is then a good measure for that in the nearest neighbour distance r_0 .

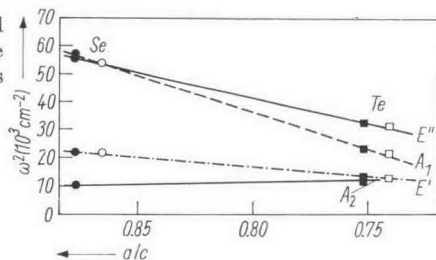
We can take therefore for the normalized interchain distance the ratio a/c , which decreases with pressure [21, 22]. This ratio also decreases from Se to Te (Table 3). Thus it seems possible to move the phonon frequencies of Se towards those of Te by applying pressure or, equivalently, by varying a/c . We plotted in Fig. 3 the squared phonon frequencies of Se and Te at zero and maximum pressure as a function of a/c . The frequencies of Te were plotted after multiplication by the ratio of the atomic mass of Te to that of Se (1.61). Since the squared eigenfrequencies of harmonic oscillators multiplied by their mass are proportional to the force constants involved, this plot gives the variation of the

Table 3

Lattice parameters of Se and Te (distances (Å))

	Se	Te
height of the hexagonal primitive cell c	4.95	5.95
interchain distance a	4.34	4.47
nearest neighbour distance r_0	2.32	2.86
valence bond angle θ	103.1°	102.6°
a/c	0.8767	0.7512
a/r_0	1.87	1.56

Fig. 3. Squared phonon frequencies of Se and Te as a function of a/c (the frequencies of Te are multiplied by the ratio of the Te:Se-masses 1.61)



mode force constants with a/c . The value of a/c at 7 kbar for Te was taken from the measurements of Jamieson and McWhan [21] performed between zero and 40 kbar. For Se only one measurement at 140 kbar of a and c was reported by McCann and Cartz [22]. The average change of a/c per kbar between zero and the maximum pressure reached is nearly the same for both materials (Se: $0.001235 \text{ kbar}^{-1}$, Te: $0.00119 \text{ kbar}^{-1}$). We therefore assumed that the change in a/c at 7 kbar is the same in Se as in Te. The straight lines connect the zero pressure points of modes of the same symmetry in Se and Te. As one can see the 7 kbar points lie also approximately on these lines. Thus, the squared phonon frequencies are to a good approximation a linear function of a/c for all data in Fig. 3.

No direct experimental information is available concerning the variation of the force constants in Se and Te with pressure. Fig. 3 shows, however, that the mode force constants vary linearly with a/c . It was pointed out above, that the dependence of a/c as a function of pressure is not known for Se but is similar to that of Te, which can be taken to be linear to within 1% in the measured range [21]. Hence Fig. 3 suggests a linear variation of mode force constants with pressure. One can therefore get an estimate of the pressure dependence of the force constants if one knows their values at $p = 0$ in Se and Te. These can be obtained from the valence force field (VFF) models which have been used for Se and Te [12, 14, 18 to 20]. These models yield values for force constants from the fit to the measured elastic constants and the $q = 0$ phonon frequencies.

We use in the following the model proposed by Nakayama and Odajima [14]. These authors represent the elastic potential energy in terms of five force constants: K_r (a bond stretching constant between nearest neighbours in the chain), K_θ (an angle bending constant between adjacent bonds), $K_{rr'}$ (a cross term of bond stretchings for the neighbouring bond pairs), $K_{r\theta}$ (a cross term of a bond stretching and an angle bending), and K_R , a force constant describing the interchain bonding. The numerical values of the force constants for Se obtained by these authors by fitting the elastic constants are given in Table 2. A similar potential was used by Nakayama et al. [20] for Te without the force constant $K_{r\theta}$. As was pointed out in [14] the large discrepancy between the calculated A_1 -mode frequency for Te (163 cm^{-1}) and the observed value (122 cm^{-1}) can be removed by introducing the term $K_{r\theta}$. Using the given values for K_r , K_R , K_θ , $K_{rr'}$ [20] and the factorized determinant of [14] we calculated the value of $K_{r\theta}$ by fitting the A_1 -mode eigenfrequency of Te to 122 cm^{-1} . The calculated frequencies for the other modes are $\omega(E'') = 141.5 \text{ cm}^{-1}$, $\omega(E') = 105.1 \text{ cm}^{-1}$, and $\omega(A_2) = 74 \text{ cm}^{-1}$. The set of force constants so obtained for Te at zero pressure is given in Table 2.

In the light of earlier remarks we assume a linear variation of these force constants with pressure. The pressure necessary to bring the zero pressure a/c value of Se to that of Te is calculated from the average value of $\Delta(a/c)/\Delta p$ ($0.00119 \text{ kbar}^{-1}$) of Te to be 110 kbar. The pressure dependence of the force constants is then given by the difference of the corresponding force constants in Se and Te divided by this pressure. These values are given in the third row of Table 2.

The following remarks can be made: K_r and K_θ decrease, while the other force constants increase with increasing pressure. K_r shows the strongest variation with pressure, which is by a factor five bigger than the variation of the other force constants. The decrease of K_r and also the increase of K_R are in agreement with the qualitative picture given by Gspan et al. [24] in terms of s and p orbitals to explain the thermal expansion of lattice parameters in Te.

Knowing the pressure dependence of the force constants we can now calculate the pressure variation of the optical phonon frequencies in Se and Te with the model of Nakayama and Odajima [14]. The calculated values are given in Table 1 together with the experimental ones. The agreement is quite good for all Raman-active frequencies, with exception of the E' -mode of Te. For Se the nearly constant E' -mode and the strong pressure dependence of the A_1 and E'' is well reproduced by the calculations. In Te the agreement for both the A_1 - and the E'' -mode is good. The strong deviation of the value for the E' -mode has to be seen as related to the fact that the calculated eigenfrequency for this mode differs also sharply from the experimental value. It has been pointed out [14] that this might be due to the strong effective charge of this mode in Te: long range electrostatic forces are, of course, not well represented in a VFF-model. In Se this effect may be less important since the effective charge is smaller [25].

As shown in Table 1 the pressure coefficient calculated for the IR-active A_2 mode is positive. This mode depends solely on the interchain constant K_R which increases upon application of pressure as the chains move together. This is also reflected in Fig. 3 where we plotted this mode for Se and Te at $p = 0$. Unfortunately, the A_2 -mode is not Raman-active and we were unable to break this selection rule by damaging the sample. The numerical calculations performed to find the pressure coefficients reveal the following facts: For Se the frequency changes of all the modes are mainly caused by the decrease of K_r . In Te all the force constants have similar influence. For the E -modes in general the contributions from the change of the different force constants have opposite sign and tend to give a smaller frequency shift. In contrast, for the A_1 -modes the main contributions add up and give the strong pressure dependence.

It might be also mentioned, that the extrapolation of the curves in Fig. 1 and 2 to higher pressure gives crosspoints for the A_1 - and E' -modes at pressures which correspond to the transition pressures to Se II (140 kbar) and Te II (40 kbar) [26, 22]. In the description of the Se-Te lattice in terms of a distorted simple Bravais lattice the A - E' splitting is caused by the distortion and should go to zero if one approaches the simple Bravais lattice. As there is no information about the pressure dependence of the angle θ (or bond length r_0), we cannot decide which structure is approached upon increasing pressure. However, simple cubic can be excluded since the a/c ratio is lower than the value $\sqrt{2/3}$ for a simple cubic lattice.

5. Conclusion

We have measured the pressure dependence of the frequencies of the first order Raman-active modes in Se and Te. The experimental results indicate that all the frequencies decrease with increasing pressure. It is shown that the application of hydrostatic pressure makes the frequencies of Se approach those of Te. This picture enabled us to calculate the change with pressure of the phonon frequencies using a valence force model proposed by Nakayama and Odajima. The calculated pressure coefficients are in reasonable agreement with the ones measured. We note that negative pressure coefficients have also been recently found in Sb for the Raman-active modes E_g and A_{1g} [27].

Acknowledgements

We would like to thank J. Arnold for the polished Te sample and G. Weiser for the Se sample. We are indebted to M. I. Bell for many stimulating discussions.

References

- [1] S. S. MITRA, C. POSTMUS, and J. R. FERRARO, Phys. Rev. Letters **18**, 455 (1967).
C. POSTMUS, J. R. FERRARO, and S. S. MITRA, Inorg. Nuclear Chem. Letters **4**, 55 (1968);
Phys. Rev. **174**, 983 (1968).
- [2] S. S. MITRA, O. BRAFMAN, W. B. DANIELS, and R. K. CRAWFORD, Phys. Rev. **186**, 942 (1969).
- [3] C. J. BUCHENAUER, F. CERDEIRA, and M. CARDONA, Proc. 2nd Internat. Conf. Light Scattering in Solids, Ed. M. BALKANSKI, Flammarion, Paris 1971 (p. 284).
- [4] A. BIENENSTOCK, Phil. Mag. **9**, 755 (1964).
- [5] G. DOLLING and R. A. COWLEY, Proc. Phys. Soc. **88**, 463 (1966).
- [6] H. JEX, phys. stat. sol. (b) **45**, 343 (1971).
- [7] R. T. PAYNE, Phys. Rev. Letters **13**, 53 (1964).
- [8] B. A. WEINSTEIN, J. B. RENUCCI, and M. CARDONA, Solid State Commun., to be published.
- [9] A. VON HIPPEL, J. chem. Phys. **16**, 372 (1948).
- [10] P. GROSSE, Springer Tracts in Modern Physics No. 48, Ed. G. HÖHLER, Springer-Verlag, Berlin 1969 (p. 59).
- [11] M. HORTAL and A. J. LEADBETTER, J. Phys. C **5**, 2129 (1972).
- [12] T. G. GIBBONS, to be published.
- [13] G. LUCOVSKY, phys. stat. sol. (b) **49**, 633 (1972).
- [14] T. NAKAYAMA and A. ODAJIMA, J. Phys. Soc. Japan **33**, 12 (1972).
- [15] D. FISCHER and P. GROSSE, Z. angew. Phys. **30**, 154 (1970).
- [16] O. BRAFMAN, S. S. MITRA, R. K. CRAWFORD, W. B. DANIELS, C. POSTMUS, and J. R. FERRARO, Solid State Commun. **7**, 449 (1969).
- [17] W. RICHTER, Proc. 11th Internat. Conf. Physics of Semiconductors Warsaw 1972, Vol. 2, Polish Sci. Publ., Warsaw 1972 (p. 1148).
- [18] M. HULIN, Proc. Internat. Conf. Lattice Dynamics, Copenhagen 1963, Pergamon Press, Oxford 1965 (p. 135).
- [19] R. GEICK, U. SCHRÖDER, and J. STUKE, phys. stat. sol. **24**, 99 (1967).
- [20] T. NAKAJAMA, Y. IKEDA, and A. ODAJIMA, J. Phys. Soc. Japan **30**, 883 (1971).
- [21] J. C. JAMIESON and D. B. MCWHAN, J. chem. Phys. **43**, 1149 (1965).
- [22] D. R. MCCANN and L. CARTZ, J. chem. Phys. **56**, 255 (1972).
- [23] J. STUKE, in: The Physics of Selenium and Tellurium, Ed. W. C. COOPER, Pergamon Press, Oxford 1969 (p. 3).
- [24] P. GSPAN, R. DROPE, and P. GROSSE, Verh. DPG **5**, 286 (1970).
- [25] G. LUCOVSKY, R. C. KEEZER, and E. BURSTEIN, Solid State Commun. **5**, 439 (1967).
- [26] F. A. BLUM, JR., and B. C. DEATON, Phys. Rev. **137**, A1410 (1965).
- [27] J. B. RENUCCI, W. RICHTER, and M. CARDONA, to be published.

(Received December 27, 1972)